

Supplementary Information

Green Fluorescent Protein Chromophore-Based Covalent Organic Polymers (GFPC-COPs): Sensing of Nitroaromatic Organic Pollutants and Explosives

Gulshan Anjum,^a Ashish Kumar,^a Ramanathan Gurunath^{a*} and Jarugu Narasimha Moorthy^{a,b,*}

^aDepartment of Chemistry, Indian Institute of Technology Kanpur, 208016, India

^bSchool of Chemistry, Indian Institute of Science Education and Research Thiruvananthapuram, Trivandrum 695551, India

*Corresponding Author; E-mail: moorthy@iitk.ac.in

CONTENTS

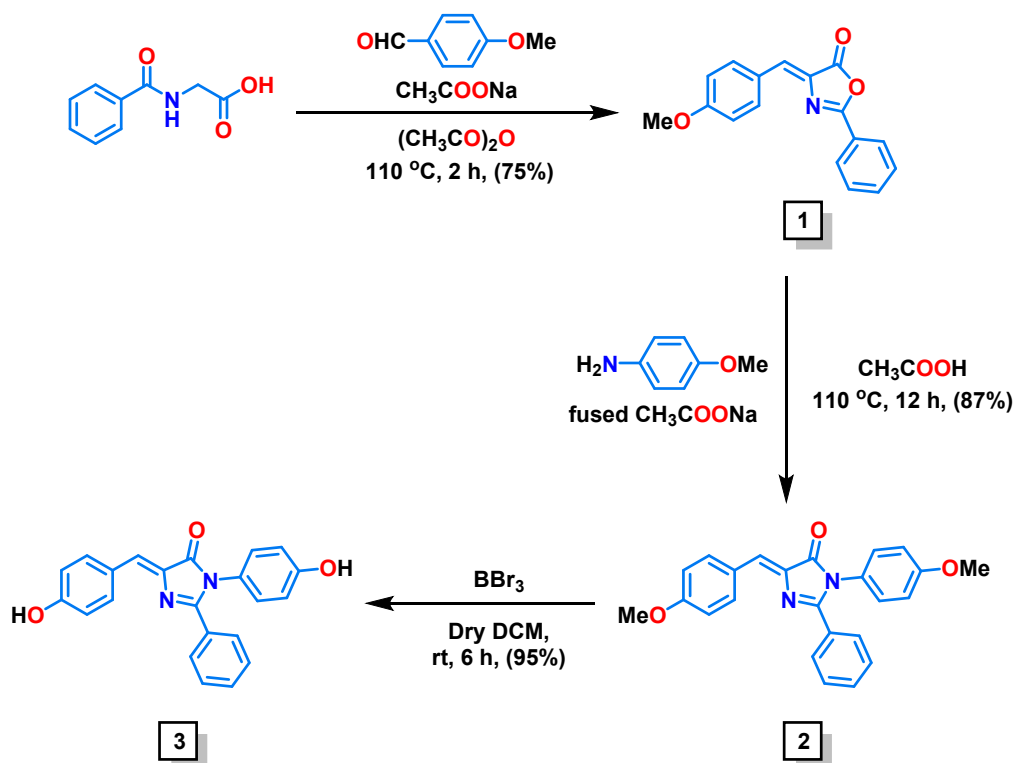
1	General aspects	S1
2	Synthesis of DHI monomer	S2-S3
3	Synthesis of THI monomer	S4-S6
4	UV-vis absorption and fluorescence emission spectra of DHI and THI in MeOH	S7
5	XPS plots of DOIDB and TOITP	S7
6	Elemental mapping of DOIDB and TOITP	S8
7	SEM-EDX analyses of DOIDB and TOITP	S8
8	Adsorption-desorption isotherms of N ₂ and CO ₂ of all four polymers	S9
9	Pore size distribution of all four polymers at 77 K and 1 bar	S10
10	IR spectra of DOIDB and TOITP before and after sonication in MeOH	S11
11	Solid-state ¹³ C NMR of DOIDB and TOITP before and after sonication in MeOH	S11
12	Emission spectra of DOIDB and TOITP in different solvents	S11
13	Fluorescence emission spectra of DOIDB and TOITP suspension with increasing concentration of nitrobenzene and trinitrotoluene (TNT)	S12
14	Fluorescence emission spectra of DOIDB and TOITP suspension with varying concentrations of aniline, phenol and thiophenol	S12
15	Sensitivity of the polymers DOIDB and TOITP to different pHs	S13
16	Fluorescence quenching spectra of DOIDB suspension with increasing concentration of NACs (nitroanilines, nitrophenols and nitrothiophenols) in methanol for excitation at 365 nm and their Stern-Volmer plots and quenching efficiencies of NACs	S13-S15

17	Fluorescence quenching spectra of TOITP suspension with increasing concentration of NACs (nitroanilines, nitrophenols and nitrothiophenols) in methanol for excitation at 370 nm and their Stern-Volmer plots and quenching efficiencies of NACs	S16-S18
18	Fluorescence quenching spectra of DMI and TMI solutions in methanol for excitation at 390 nm with TNP and corresponding Stern-Volmer plots and quenching efficiencies of DMI , TMI , DOIDB and TOIDB	S19
19	UV-vis absorption spectra of equimolar concentrations of TNT and TNP in MeOH	S20
20	Selective absorption of TNP over TNT by TOITP polymer in a solution containing equimolar concentrations of TNT and TNP in MeOH at different time intervals	S20
21	Comparison of the performances of DOIDB and TOITP polymers in sensing of 4-nitroaniline and TNP with those of other materials reported previously in the literature	S21-S24
22	NMR spectra of all compounds	S25-S27
23	References	S28

General aspects

All reagents, available from commercial sources, were used without further purification. Freshly distilled solvents were used for the synthesis. Column chromatography was performed by using silica gel of 100–200 mesh for the purification of compounds. ^1H and ^{13}C NMR spectra were recorded on 400 MHz and 500 MHz JEOL-Lambda spectrometers. IR spectra were recorded on a Bruker Vector 22 FT-IR spectrometer. High-resolution mass spectra (HRMS) were recorded on an ESI-QToF (Agilent 6546) instrument. Thermogravimetric analyses were carried out with an SDT-Q600TGA apparatus under an N_2 atmosphere with a heating rate of $10\text{ }^\circ\text{C min}^{-1}$. Melting points were determined using a PERFIT melting point apparatus. The gas sorption analyses were performed by a Quantachrome Autosorb iQ automated gas sorption analyser for BET surface area. The average pore size and pore size distributions were determined by the NLDFT method using the nitrogen sorption isotherms. Scanning electron microscope (SEM) images were recorded on a Nova Nano SEM 450. AFM images were recorded in the tapping mode using an Asylum Research atomic force microscope (AC240TS-R3, Oxford Instruments Company); all measurements were carried out under ambient conditions using a silicon cantilever coated with Al (100) with a resonance frequency of 70 kHz and a force constant of 2 N m^{-1} and the images were processed using Gwyddion software (version 2.4). HR-TEM images were recorded on carbon-coated Cu grids with FEI Titan G2 60-300 HRTEM, operating at a voltage of 300 kV. XPS analyses were carried out with X-ray photoelectron spectroscopy module, PHI 5000 Versa Prob II, FEI Inc. Steady-state fluorescence measurements were carried out using a FluoroMax-4 spectrophotometer (Horiba Jobin Yvon Technology). Fluorescence quantum yields were determined using a ‘Quanta- ϕ : F-3029’ integrating sphere (Horiba Scientific; sphere inner diameter = 150 mm) connected to the spectrofluorimeter via optical fibres. The emission spectra for dispersed suspensions were recorded using a 3.0 mL cuvette. HPLC-grade solvents were employed for all studies.

Synthesis of DHI monomer



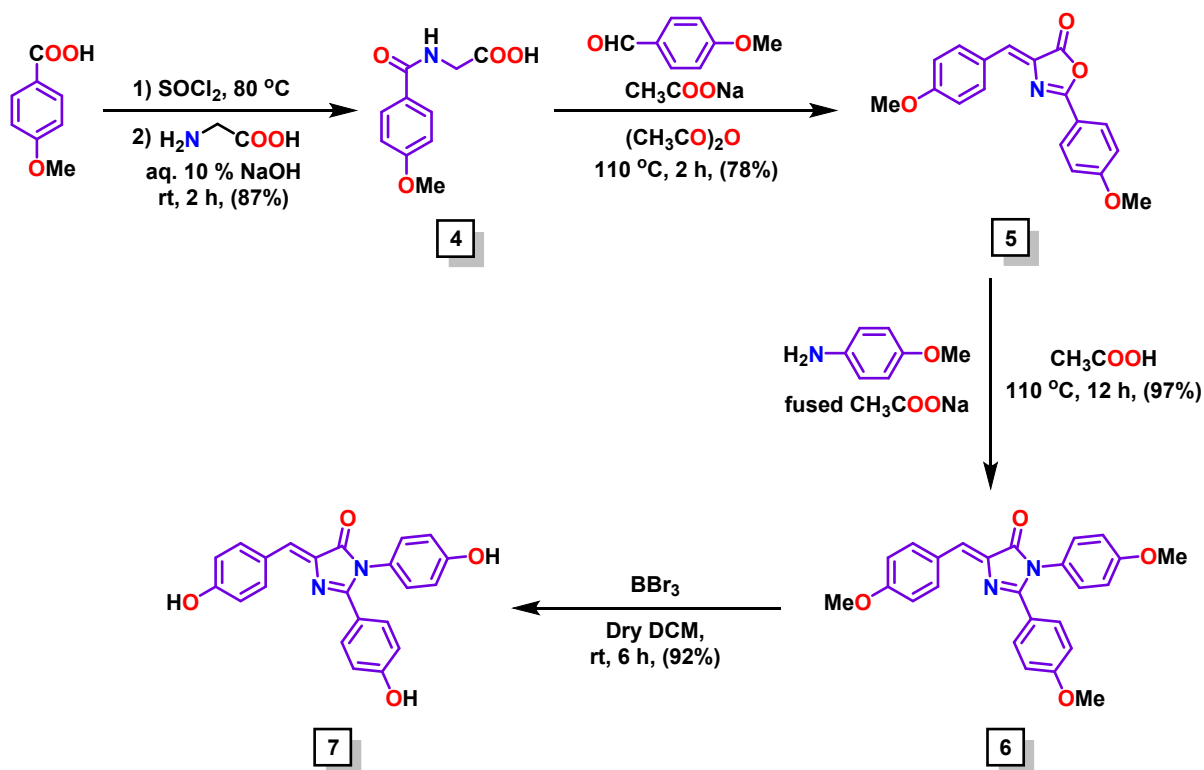
Scheme S1: Synthesis of DHI monomer.

Synthesis of (Z)-4-(4-methoxybenzylidene)-2-phenyloxazol-5(4H)-one (1).¹ An oven-dried round-bottomed flask was charged with hippuric acid (1.0 g, 5.6 mmol), anisaldehyde (0.68 mL, 5.6 mmol), anhyd. sodium acetate (0.46 g, 5.6 mmol) and acetic anhydride (2.1 mL, 22.3 mmol). The resulting suspension was heated at $240\text{ }^\circ\text{C}$ with constant stirring until all solids were dissolved and a clear solution resulted. Subsequently, the reaction mixture was maintained at $100\text{ }^\circ\text{C}$ and the stirring was continued at this temperature for 2 h. After completion of the reaction, it was cooled to rt and 3 mL of ethanol was added slowly to the contents of the flask. The mixture was allowed to stand overnight and the resulting precipitate was filtered, and washed with cold ethanol and distilled water. The material thus obtained was dried in an oven at $80\text{ }^\circ\text{C}$ and the desired product was isolated as a yellow solid in 75% yield (1.17 g). $^1\text{H NMR}$ (400 MHz, CDCl_3) δ 3.88 (s, 3H), 6.99 (d, $J = 8.8\text{ Hz}$, 2H), 7.21 (s, 1H), 7.51 (dd, $J = 7.2\text{ Hz}$, 8 Hz, 2H), 7.58 (dd, $J = 7.6\text{ Hz}$, 7.2 Hz, 1H), 8.15-8.19 (m, 4H).

Synthesis of (Z)-4-(4-methoxybenzylidene)-1-(4-methoxyphenyl)-2-phenyl-5-imidazolinone (2). Compound **2** was synthesized by slightly modifying the procedure reported in the literature.¹ In a round-bottomed flask, (Z)-4-(4-methoxybenzylidene)-2-phenyloxazol-5(4H)-one (1.0 g, 3.6 mmol), *p*-anisidine (0.53 g, 4.3 mmol), and anhyd. sodium acetate (0.59 g, 7.2 mmol) were dissolved in CH₃COOH (10 mL) and heated at 110 °C for 12 h. The progress of the reaction was monitored by TLC. After completion of the reaction, the reaction mixture was cooled to rt, ethanol (10 mL) was slowly added to the reaction mixture and it was kept in the fridge overnight to precipitate out the product. The precipitate obtained was filtered, washed with a minimum amount of EtOH and plenty of water to remove the acid. It was subsequently dried in an oven at 80 °C to obtain the required product, (Z)-5-(4-methoxybenzylidene)-3-(4-methoxyphenyl)-2-phenyl-3,5-dihydro-4H-imidazol-4-one (**2**), as a yellow solid material in 87% yield (1.2 g). ¹H NMR (400 MHz, CDCl₃) δ 3.82 (s, 3H), 3.86 (s, 3H), 6.92 (d, *J* = 9.2 Hz, 2H), 6.97 (d, *J* = 8.4 Hz, 2H), 7.09 (d, *J* = 8.8 Hz, 2H), 7.28-7.32 (m, 3H), 7.4 (dd, *J* = 7.2 Hz, 7.6 Hz, 1H), 7.58 (d, *J* = 7.2 Hz, 2H), 8.26 (d, *J* = 9.2 Hz, 2H).

Synthesis of (Z)-4-(4-hydroxybenzylidene)-1-(4-hydroxyphenyl)-2-phenyl-5-imidazolinone (3). To a solution of (Z)-5-(4-methoxybenzylidene)-3-(4-methoxyphenyl)-2-phenyl-3,5-dihydro-4H-imidazol-4-one (1.0 g, 2.6 mmol) in 30 mL of dry DCM contained in a round bottom flask, BBr₃ (0.62 mL, 6.5 mmol) was added dropwise under N₂ atmosphere. The reaction mixture was stirred at rt for 6 h. After completion of the reaction, the reaction mixture was quenched with ice, and the solvent was removed in vacuo. The organic material was extracted with CHCl₃ three times and the combined extract was dried over Na₂SO₄. The solvent was removed and the resulting crude residue was subjected to silica-gel column chromatography using EtOAc/CHCl₃/pet ether as an eluent to afford the pure product, that is, (Z)-5-(4-hydroxybenzylidene)-3-(4-hydroxyphenyl)-2-phenyl-3,5-dihydro-4H-imidazol-4-one (**3**), as a yellow solid in 95% yield (0.88 g). mp >250 °C; IR (KBr) cm⁻¹ 3361, 2942, 1690, 1595, 1445, 1384, 1242, 1173; ¹H NMR (400 MHz, DMSO-*d*₆) δ 6.76 (d, *J* = 8.4 Hz, 2H), 6.84 (d, *J* = 8.4 Hz, 2H), 7.0 (d, *J* = 8.4 Hz, 2H), 7.11 (s, 1H), 7.33 (dd, *J* = 7.2 Hz, 7.6 Hz, 2H), 7.42 (dd, *J* = 7.2 Hz, 7.6 Hz, 1H), 7.49 (d, *J* = 7.6 Hz, 2H), 8.18 (d, *J* = 9.2 Hz, 2H), 9.73 (bs, 1H), 10.21 (bs, 1H); ¹³C NMR (125 MHz, DMSO-*d*₆) δ 116.3, 116.5, 126, 126.3, 128.7, 128.8, 129.3, 129.5, 129.6, 131.5, 135.2, 136.2, 157.9, 159.6, 160.7, 170.6; ESI-MS *m/z* calculated for C₂₂H₁₇N₂O₃ 357.1239 [M + H]⁺, found 357.1232.

Synthesis of THI monomer



Scheme S2: Synthesis of THI monomer.

Synthesis of (4-methoxybenzoyl)glycine (4).^{2,3} In an oven-dried round-bottomed flask, 4-methoxybenzoic acid (1.0 g, 6.6 mmol) was dissolved in SOCl_2 (1 mL, 13.1 mmol) under an N_2 atmosphere and heated at 80 °C for 3 h. After the formation of 4-methoxybenzoyl chloride, the temperature was raised to 90 °C and SOCl_2 was removed. The light pink liquid thus obtained as a product, slowly solidified as a light-pink material at rt.

A solution of glycine (0.5 g, 6.6 mmol) in 10% NaOH (5 mL) was added to 4-methoxybenzoyl chloride with vigorous stirring. The reaction was continued at rt for two more hours. Subsequently, ice was added to the reaction mixture followed by 2 mL of Conc. HCl, leading to the formation of a precipitate. The latter was filtered, washed thoroughly with water and dried in an oven. Pure 4-methoxybenzoyl glycine (4) was obtained as a colourless solid material in 87% yield (1.2 g). ^1H NMR (400 MHz, $\text{DMSO}-d_6$) δ 3.76 (s, 3H), 3.86 (d, $J = 6$ Hz, 2H), 6.96 (d, $J = 8.8$ Hz, 2H), 7.80 (d, $J = 8.4$ Hz, 2H), 8.63 (t, $J = 6$ Hz, 5.6 Hz, 1H), 12.51 (s, 1H).

Synthesis of (Z)-4-(4-methoxybenzylidene)-2-(4-methoxyphenyl)oxazol-5(4H)-one (5).³

An oven-dried round-bottomed flask was charged with 4-methoxybenzoyl glycine (1.0 g, 4.8 mmol), anisaldehyde (0.58 mL, 4.8 mmol), anhyd. sodium acetate (0.39 g, 4.8 mmol) and acetic anhydride (2.3 mL, 24 mmol). The resulting suspension was heated at 240 °C with constant stirring until all solids got dissolved and converted into a clear solution. Subsequently, the reaction mixture was heated at 100 °C for 2 h. After completion of the reaction, it was cooled to rt and 3 mL of ethanol was added slowly to the contents of the flask. The mixture was allowed to stand overnight, and the resulting precipitate was filtered, washed with cold ethanol followed by distilled water and dried in an oven at 80 °C. The desired product **5** was isolated as a yellow solid in 78% yield (1.15 g). ¹H NMR (500 MHz, CDCl₃) δ 3.88 (s, 3H), 3.89 (s, 3H), 6.99 (dd, *J* = 9 Hz, 9 Hz, 4H), 7.15 (s, 1H), 8.11 (d, *J* = 9 Hz, 2H), 8.17 (d, *J* = 8.5 Hz, 2H).

Synthesis of (Z)-4-(4-methoxybenzylidene)-1,2-bis(4-methoxyphenyl)-5-imidazolinone (6).

In a round-bottomed flask, (Z)-4-(4-methoxybenzylidene)-2-(4-methoxyphenyl)oxazol-5(4H)-one (1.0 g, 3.2 mmol), *p*-anisidine (0.48 g, 3.9 mmol), and anhyd. sodium acetate (0.53 g, 6.4 mmol) were dissolved in CH₃COOH (10 mL) and heated at 110 °C for 12 h. The reaction was monitored by TLC. At the end of the reaction, ethanol (10 mL) was slowly added to the reaction mixture and allowed to stand overnight. The precipitate obtained was filtered, washed thoroughly with EtOH and plenty of water to remove the acid. It was subsequently dried in an oven at 80 °C to obtain the desired product, that is, (Z)-5-(4-methoxybenzylidene)-2,3-bis(4-methoxyphenyl)-3,5-dihydro-4H-imidazol-4-one (**6**), as a yellow solid material in 97% yield (1.3 g); mp = 204 °C; IR (KBr) cm⁻¹ 3010, 2930, 1709, 1640, 1596, 1513, 1162; ¹H NMR (400 MHz, CDCl₃) δ 3.8 (s, 3H), 3.83 (s, 3H), 3.86 (s, 3H), 6.81 (d, *J* = 9.2 Hz, 2H), 6.95 (dd, *J* = 9.2 Hz, 9.2 Hz, 4H), 7.10 (d, *J* = 9.2 Hz, 2H), 7.22 (s, 1H), 7.54 (d, *J* = 9.2 Hz, 2H), 8.25 (d, *J* = 9.2 Hz, 2H); ¹³C NMR (125 MHz, CDCl₃) δ 55.45, 55.48, 55.58, 113.8, 114.4, 114.8, 121.3, 127.6, 127.8, 128.2, 128.8, 131.1, 134.5, 136.8, 159.1, 159.4, 161.4, 162, 171.1; ESI-MS *m/z* calculated for C₂₅H₂₃N₂O₄ 415.1658 [M + H]⁺, found 415.1660.

Synthesis of (Z)-4-(4-hydroxybenzylidene)-1,2-bis(4-hydroxyphenyl)-5-imidazolinone (7).

To a solution of (Z)-5-(4-methoxybenzylidene)-2,3-bis(4-methoxyphenyl)-3,5-dihydro-4H-imidazol-4-one (1.0 g, 2.4 mmol) in 30 mL of dry DCM contained in a round bottom flask was added BBr₃ (1 mL, 10.8 mmol) dropwise under N₂ atmosphere. The reaction mixture was stirred at rt for 6 h. After completion of the reaction, the reaction mixture was quenched with ice, and the solvent was removed in vacuo. The organic material thus obtained was extracted with CHCl₃ three times and the combined extract was dried over Na₂SO₄. The solvent was removed in vacuo, and the crude product residue was purified by silica-gel column chromatography using EtOAc:Pet. ether (50:50) as the eluent. The pure product (Z)-5-(4-hydroxybenzylidene)-2,3-bis(4-hydroxyphenyl)-3,5-dihydro-4H-

imidazol-4-one (7) was obtained as a yellow solid in 92% yield (0.83 g). mp >250 °C; IR (KBr) cm^{-1} 3387, 2930, 1653, 1578, 1503, 1442, 1163; ^1H NMR (400 MHz, $\text{DMSO-}d_6$) δ 6.68 (d, $J = 8$ Hz, 2H), 6.80 (dd, $J = 8.4$ Hz, 8 Hz, 4H), 6.98-6.99 (m, 3H), 7.34 (d, $J = 8$ Hz, 2H), 8.15 (d, $J = 8$ Hz, 2H), 9.74 (bs, 1H), 10.13 (bs, 2H); ^{13}C NMR (125 MHz, $\text{DMSO-}d_6$) δ 115.7, 116.4, 119.9, 126.3, 126.7, 126.9, 129.7, 131.3, 134.9, 136.5, 157.9, 159.4, 160.3, 160.8, 170.9; ESI-MS m/z calculated for $\text{C}_{22}\text{H}_{17}\text{N}_2\text{O}_4$ 373.1188 $[\text{M} + \text{H}]^+$, found 373.1189.

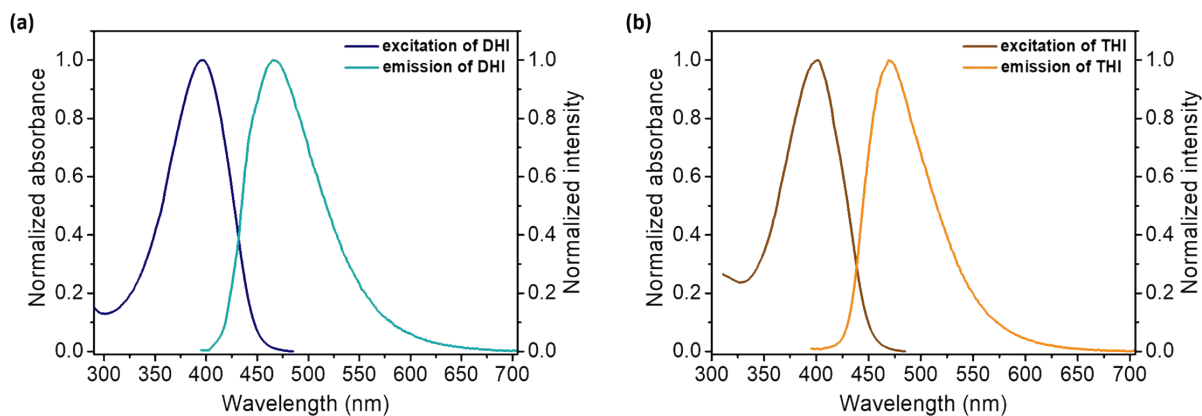


Fig. S1 (a, b) UV-vis absorption and fluorescence emission spectra of **DHI** and **THI** in MeOH, respectively; **DHI** and **THI** were excited at 395 and 400 nm, respectively.

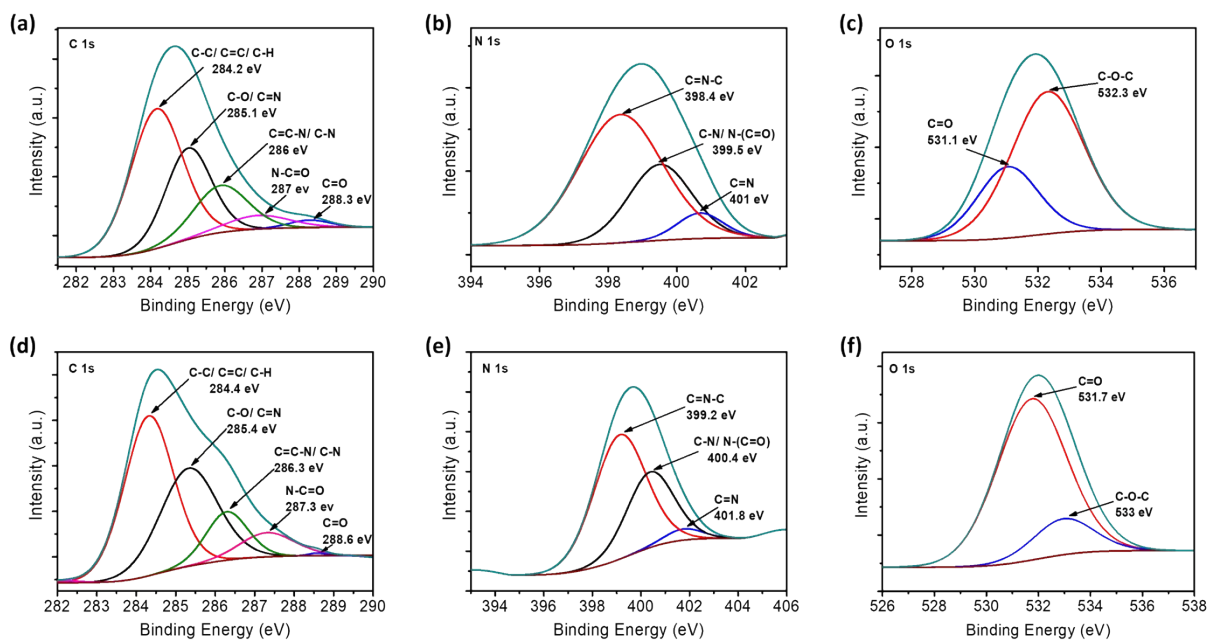


Fig. S2 (a, b and c) XPS plots of **DOIDB**. (d, e and f) XPS plots of **TOITP**.

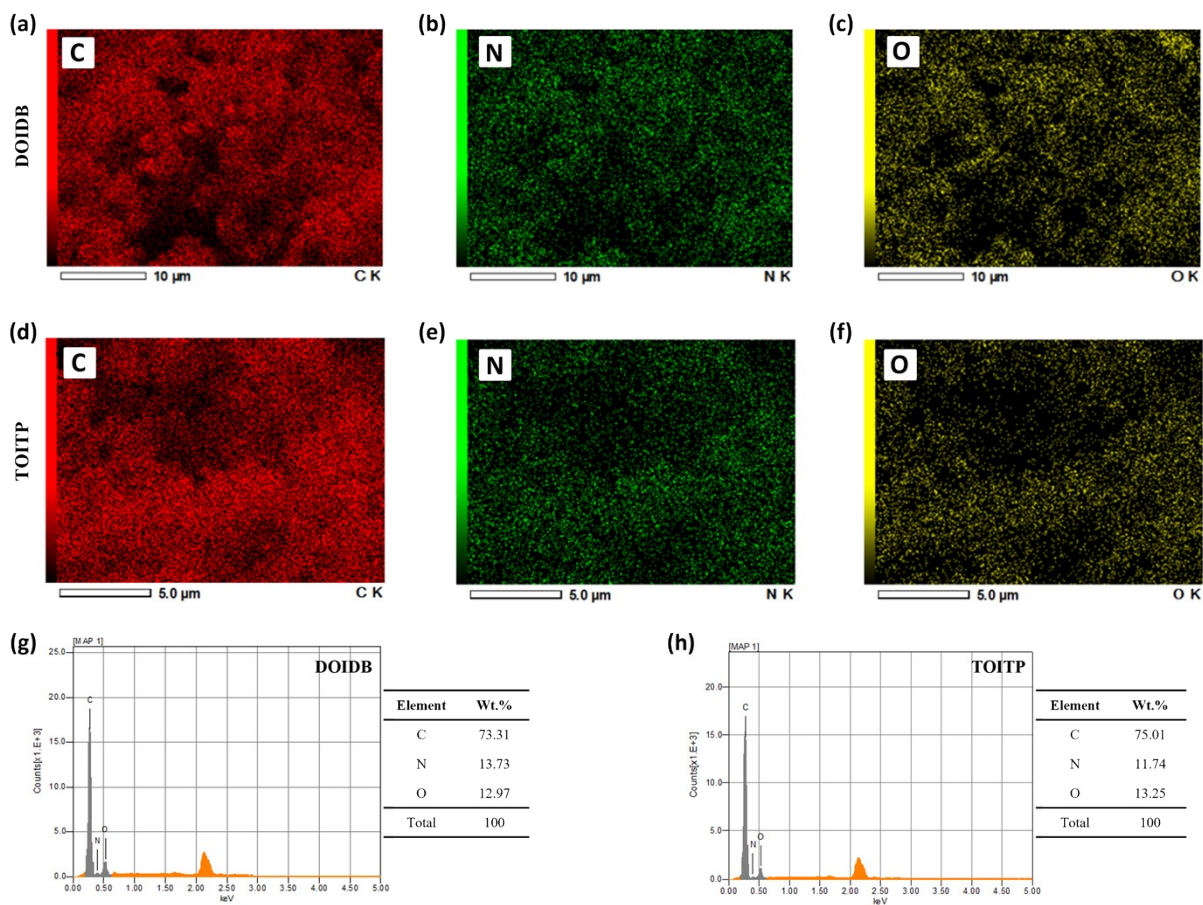


Fig. S3 (a, b and c) Elemental mapping of **DOIDB**. (d, e and f) Elemental mapping of **TOITP**. (g, h) SEM-EDX analyses of **DOIDB** and **TOITP**, respectively.

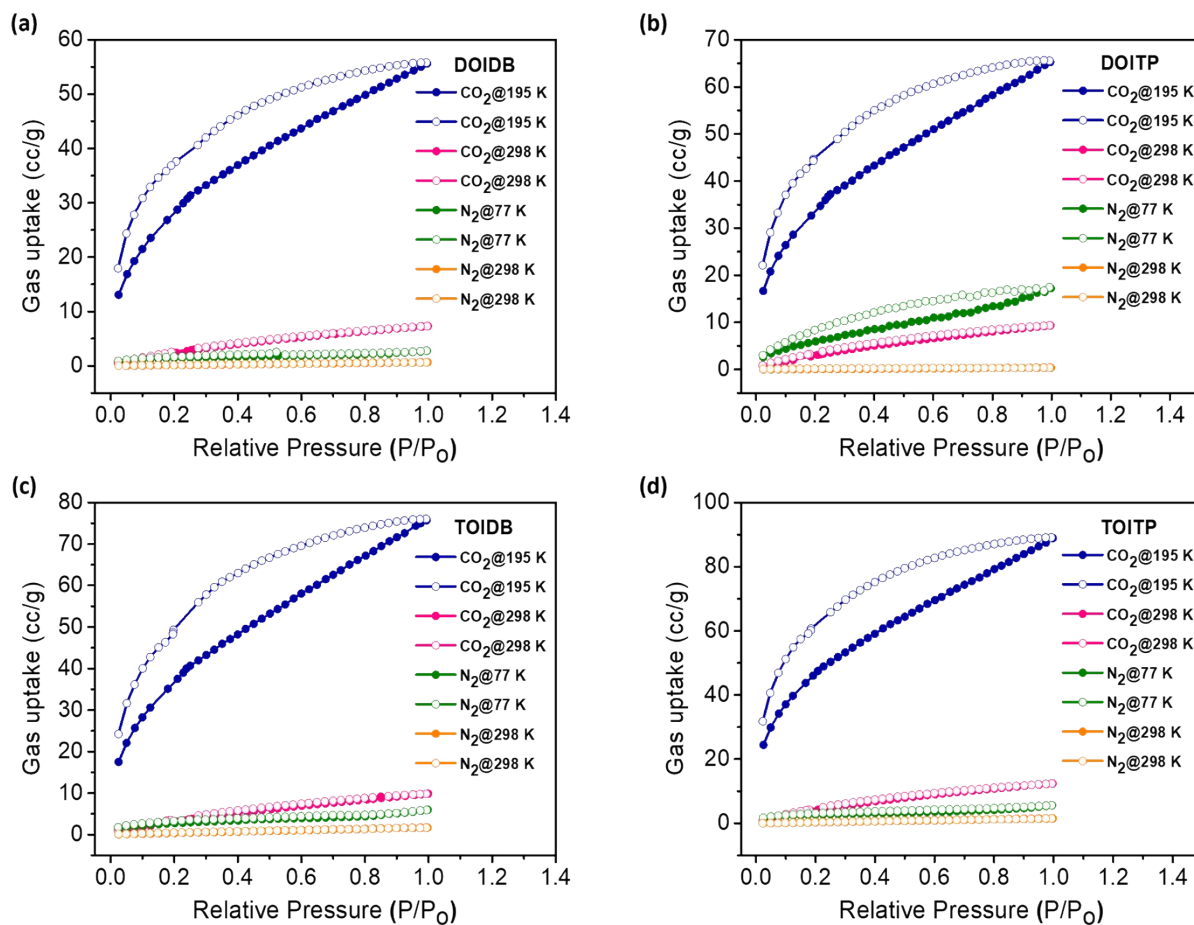


Fig. S4 (a-d) Adsorption-desorption isotherms of N_2 and CO_2 of all four polymers. Filled and open circles represent the adsorption and desorption profiles, respectively.

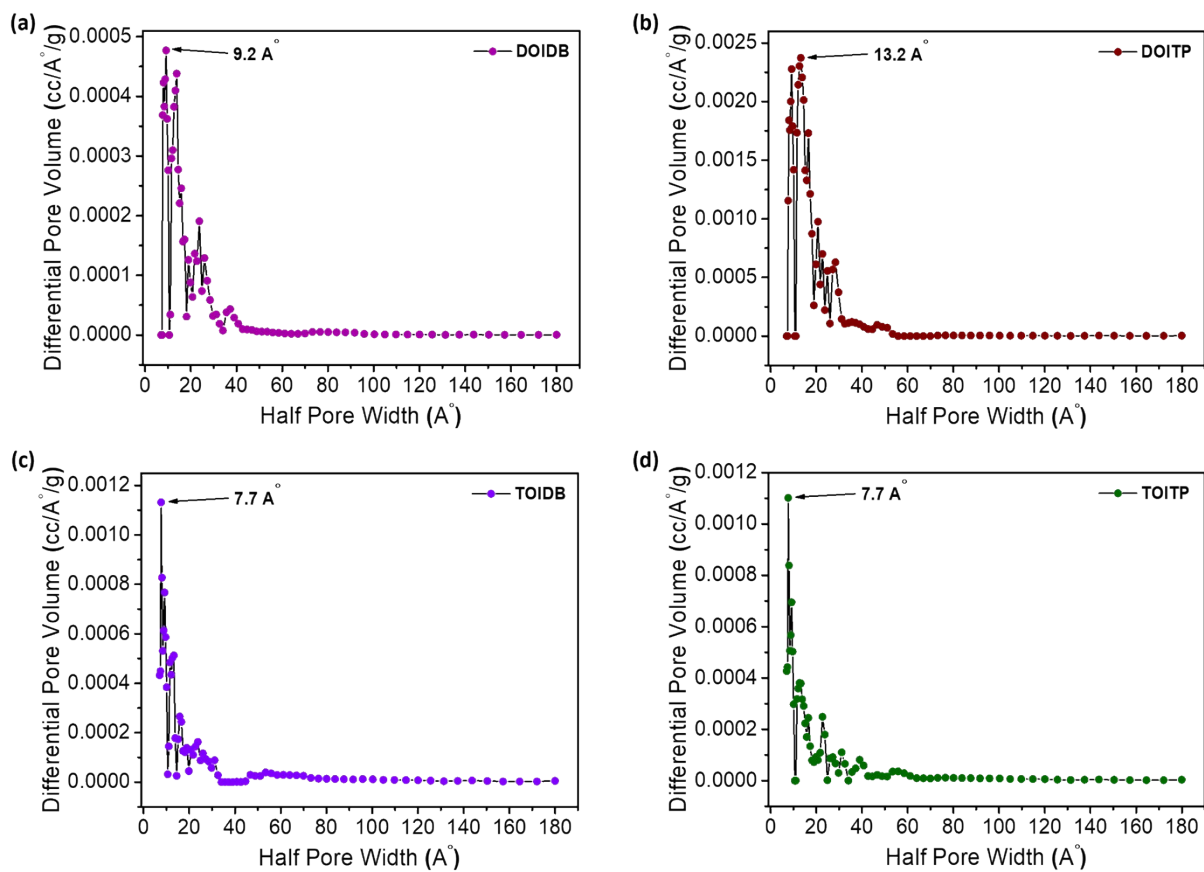


Fig. S5 (a-d) Pore size distribution of all four polymers at 77 K and 1 bar.

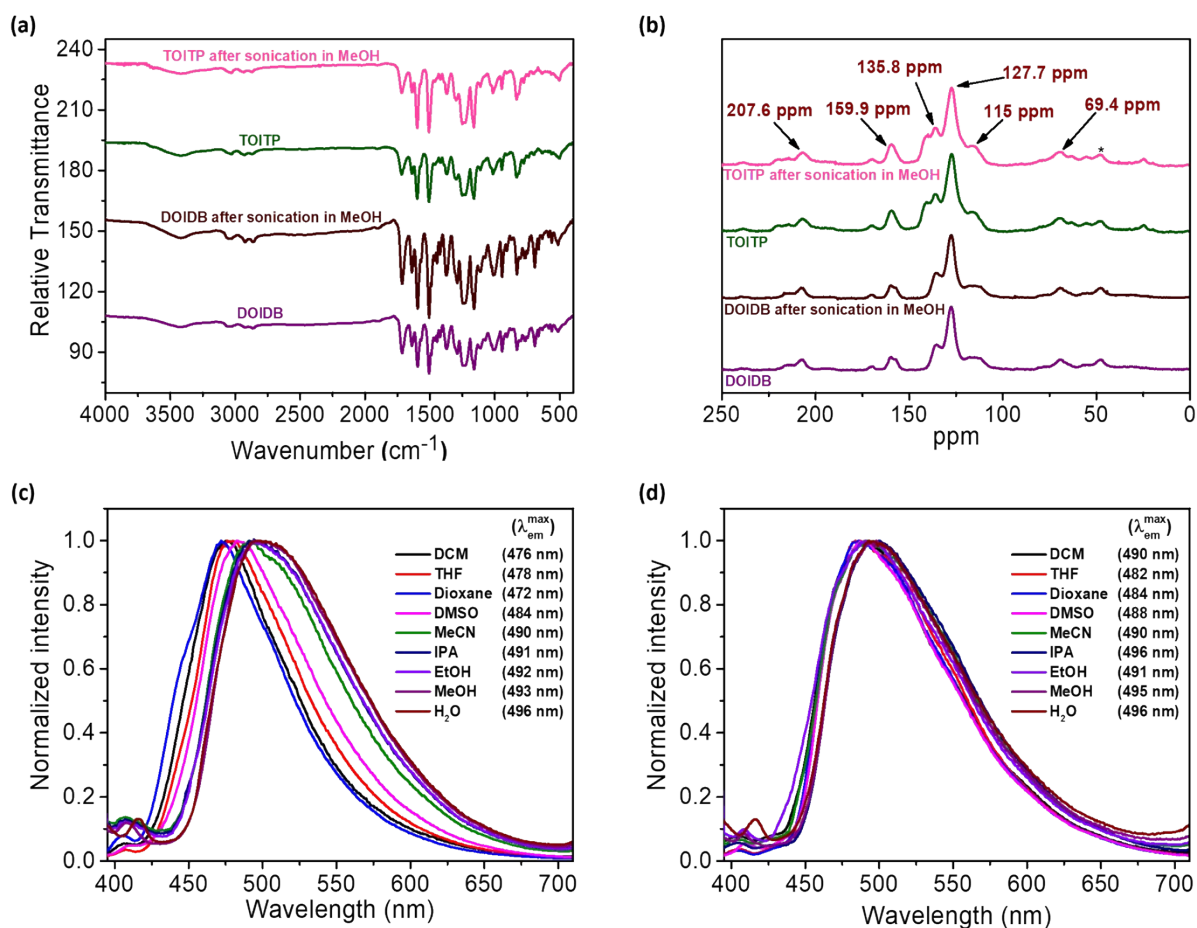


Fig. S6 (a) IR spectra of **DOIDB** and **TOITP** before and after sonication in MeOH. (b) Solid-state ¹³C NMR of **DOIDB** and **TOITP** before and after sonication in MeOH. (c) Emission spectra of **DOIDB** in different solvents. (d) Emission spectra of **TOITP** in different solvents.

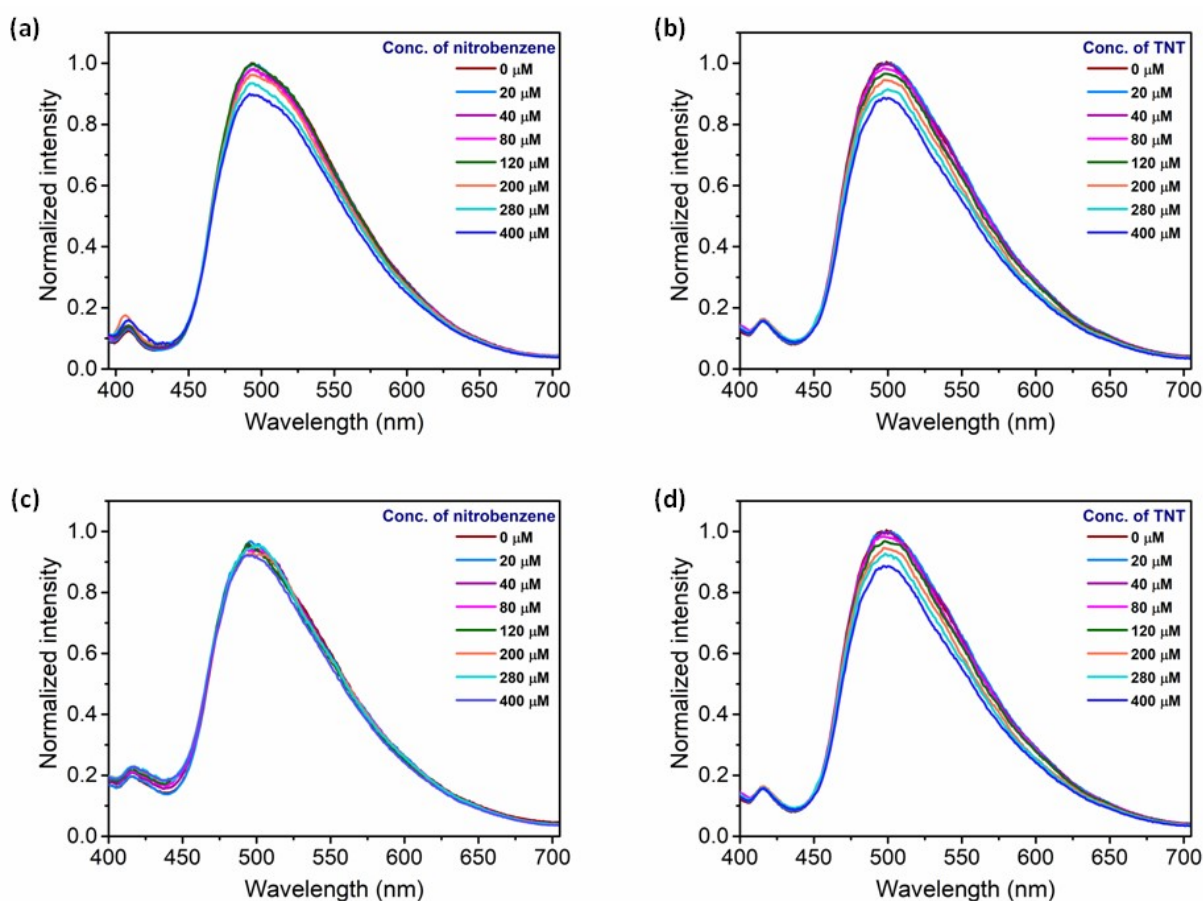


Fig. S7 (a,b) Fluorescence emission spectra of **DOIDB** suspension with increasing concentration of nitrobenzene and trinitrotoluene (TNT). (c,d) Fluorescence emission spectra of **TOITP** suspension with increasing concentration of nitrobenzene and trinitrotoluene (TNT).

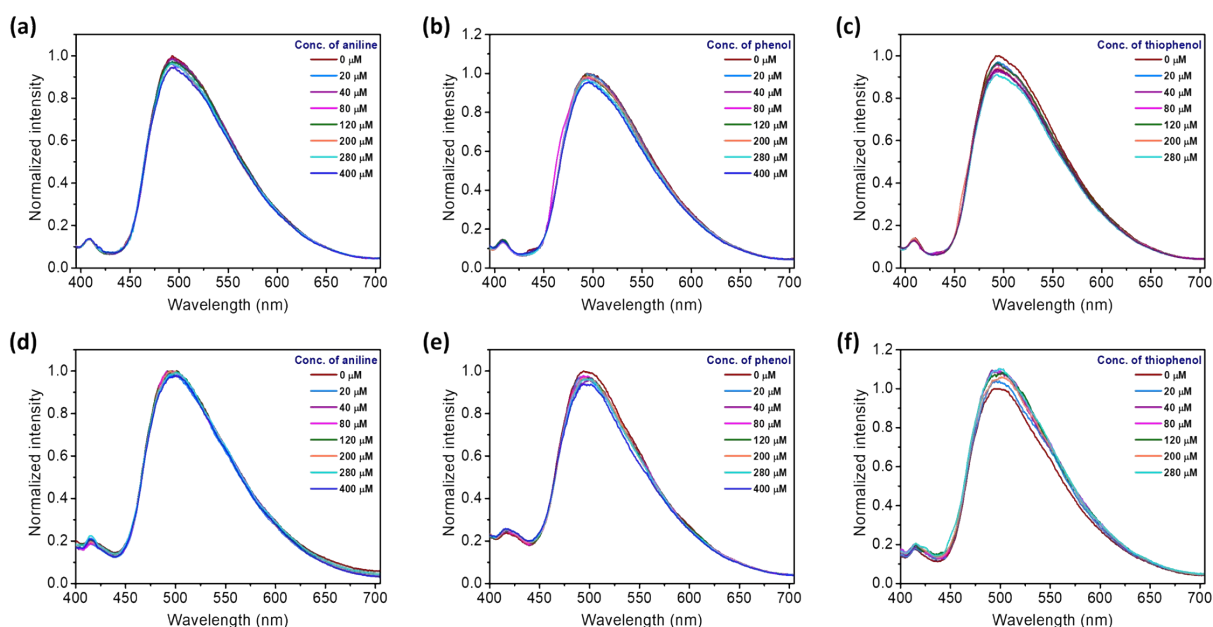


Fig. S8 (a, b and c) Fluorescence emission spectra of **DOIDB** suspension with varying concentrations of aniline, phenol and thiophenol. (d, e and f) Fluorescence emission spectra of **TOITP** suspension with varying concentrations of aniline, phenol and thiophenol.

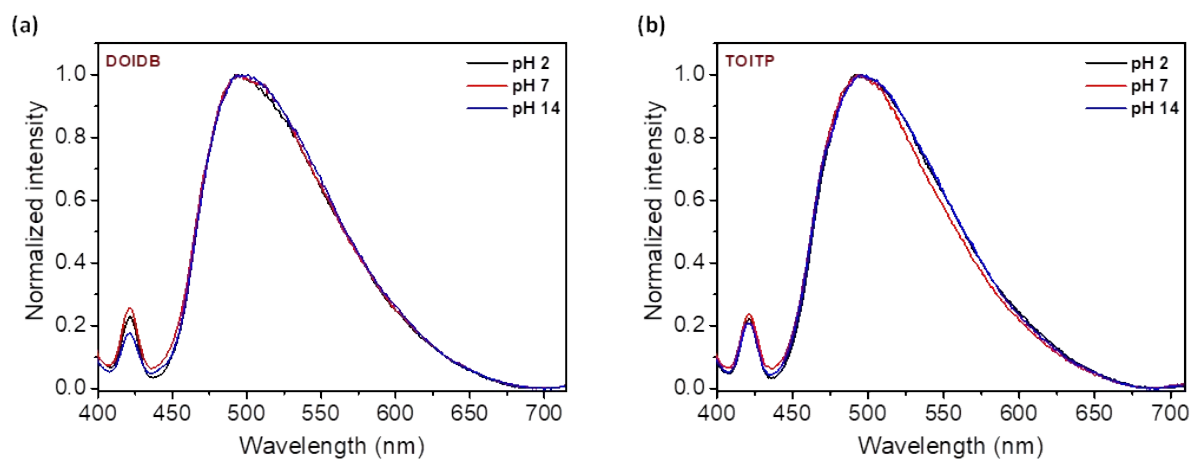


Fig. S9 (a) and (b) Sensitivity of the polymers **DOIDB** and **TOITP** to different pHs, respectively, by making suspension of 1 mg of each polymer in 10 mL of milli-Q water at three different pHs.

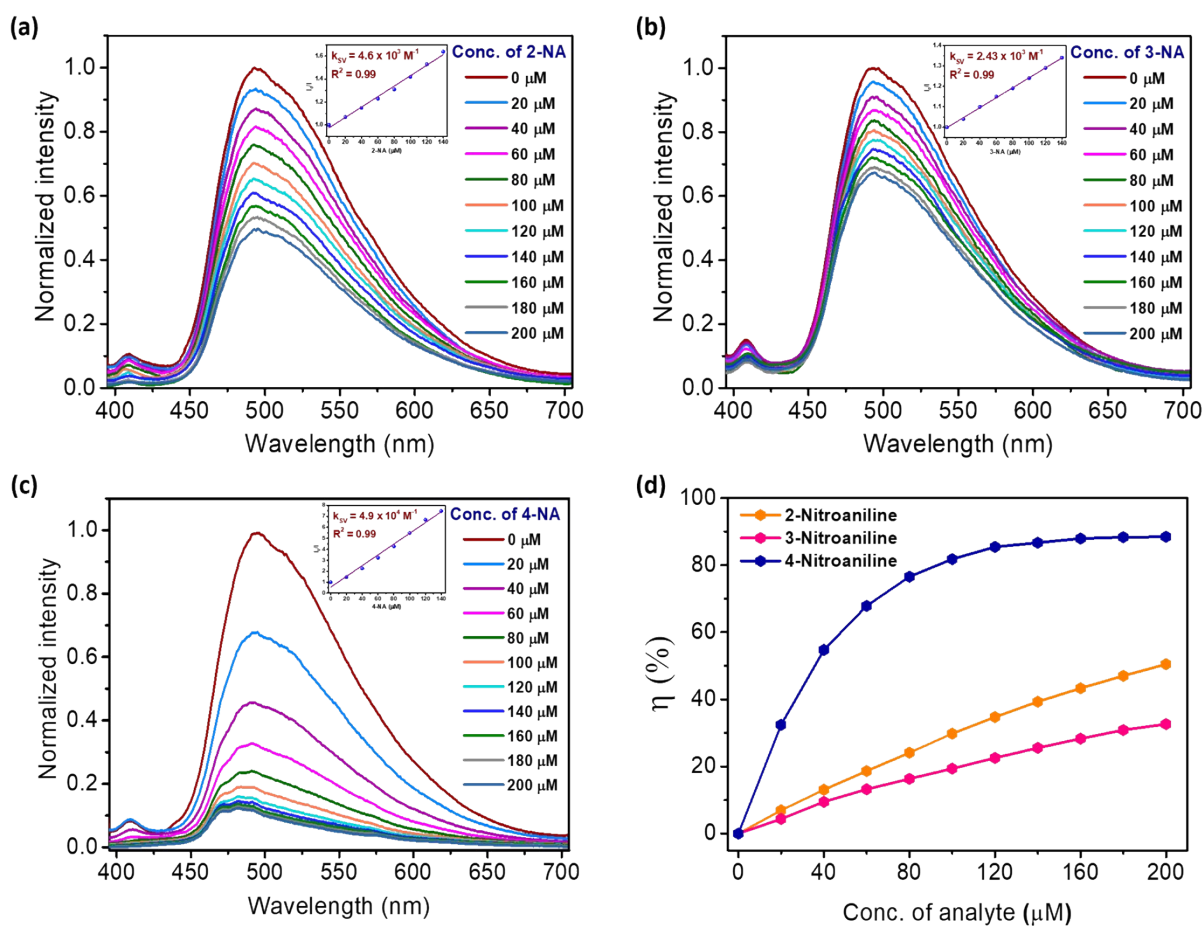


Fig. S10 Fluorescence quenching spectra of **DOIDB** suspension with increasing concentrations of nitroanilines (NAs) in methanol for excitation at 365 nm and their Stern-Volmer plots, (a) 2-nitroaniline (2-NA), (b) 3-nitroaniline (3-NA), (c) 4-nitroaniline (4-NA). (d) Quenching efficiencies of NAs.

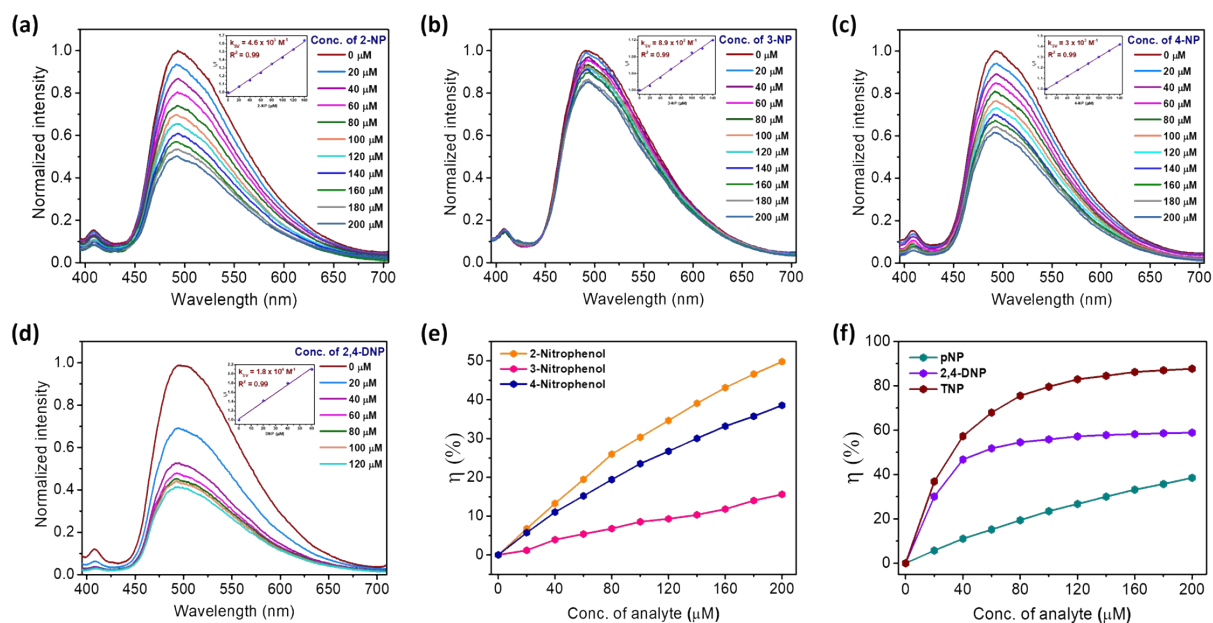


Fig. S11 Fluorescence quenching spectra of **DOIDB** suspension with increasing concentrations of nitrophenols (NPs) in methanol for excitation at 365 nm and their Stern-Volmer plots, (a) 2-nitrophenol (2-NP), (b) 3-nitrophenol (3-NP), (c) 4-nitrophenol (4-NP), and (d) 2,4-dinitrophenol (2,4-DNP). (e,f) Quenching efficiencies of NPs.

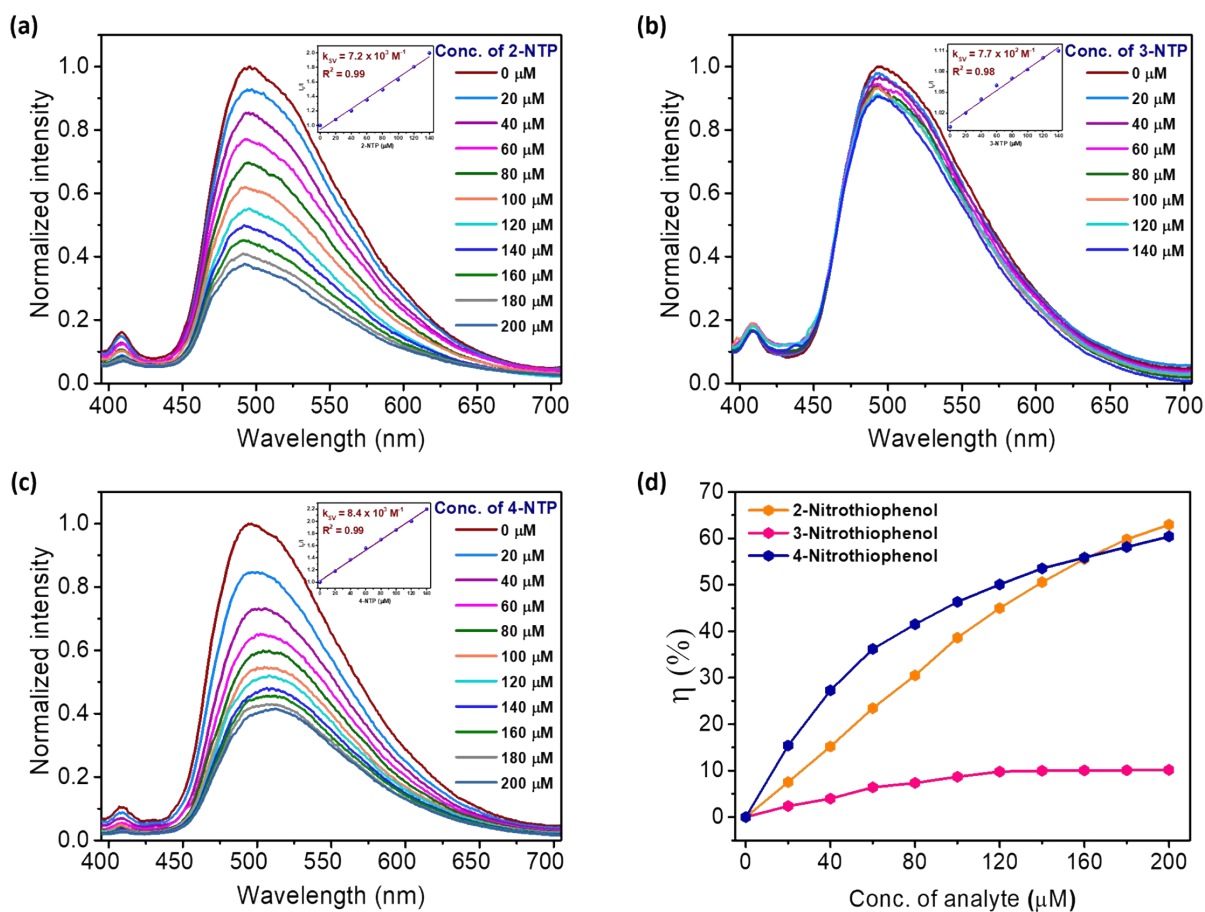


Fig. S12 Fluorescence quenching spectra of **DOIDB** suspension with increasing concentrations of nitrothiophenols (NTPs) in methanol for excitation at 365 nm and their Stern-Volmer plots, (a) 2-nitrothiophenol (2-NTP), (b) 3-nitrothiophenol (3-NTP), and (c) 4-nitrothiophenol (4-NTP). (d) Quenching efficiencies of NTPs.

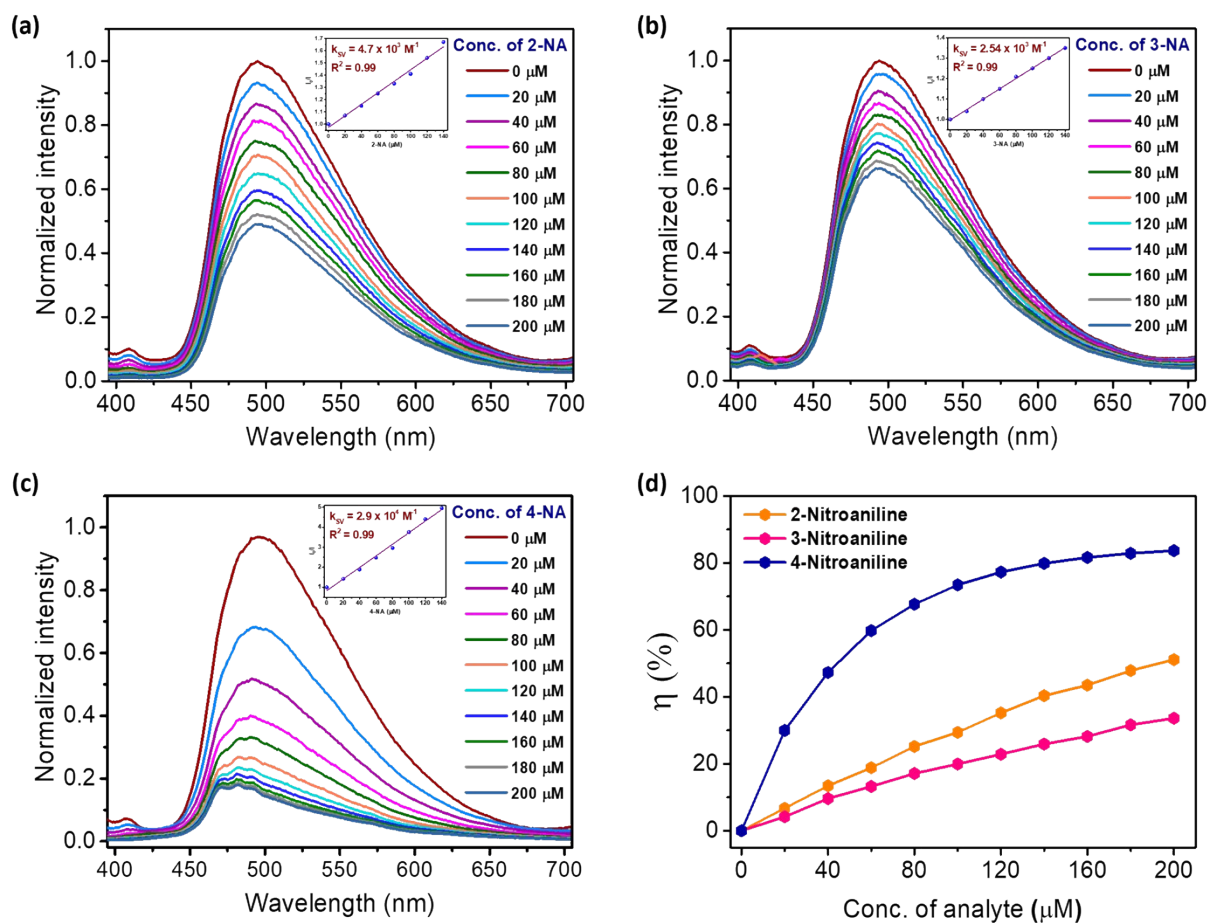


Fig. S13 Fluorescence quenching spectra of TOITP suspension with increasing concentrations of nitroanilines (NAs) in methanol for excitation at 370 nm and their Stern-Volmer plots, (a) 2-nitroaniline (2-NA), (b) 3-nitroaniline (3-NA), and (c) 4-nitroaniline (4-NA). (d) Quenching efficiencies of NAs.

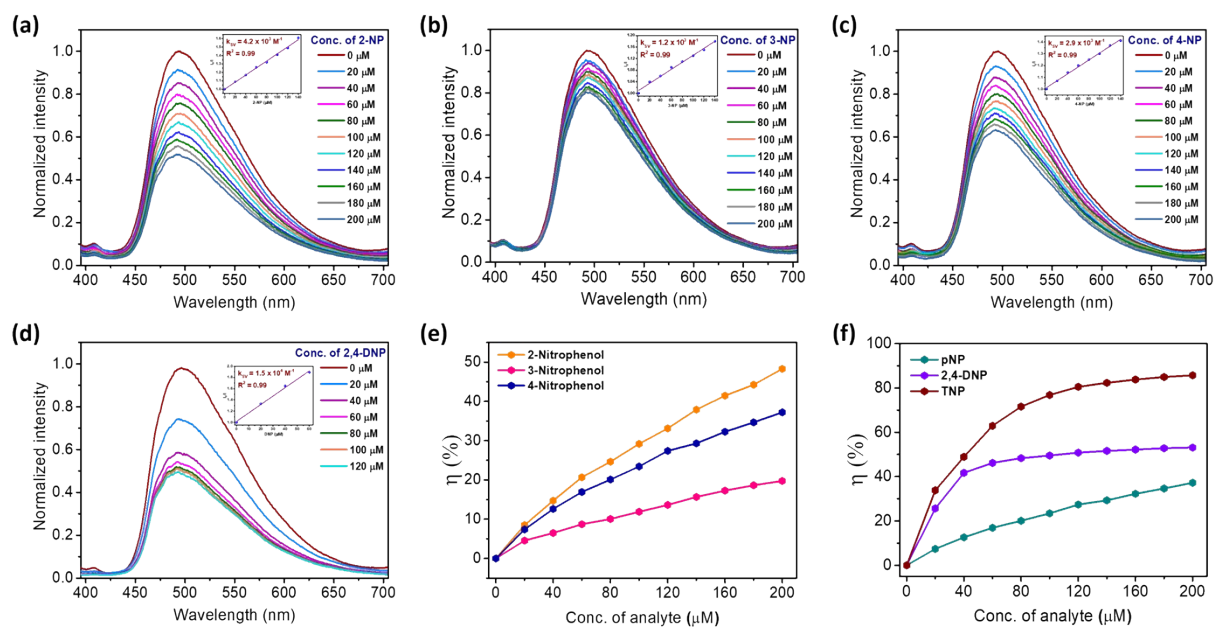


Fig. S14 Fluorescence quenching spectra of **TOITP** suspension with increasing concentrations of nitrophenols (NPs) in methanol for excitation at 370 nm and their Stern-Volmer plots, (a) 2-nitrophenol (2-NP), (b) 3-nitrophenol (3-NP), (c) 4-nitrophenol (4-NP), and (d) 2,4-dinitrophenol (2,4-DNP). (e and f) Quenching efficiencies of NPs.

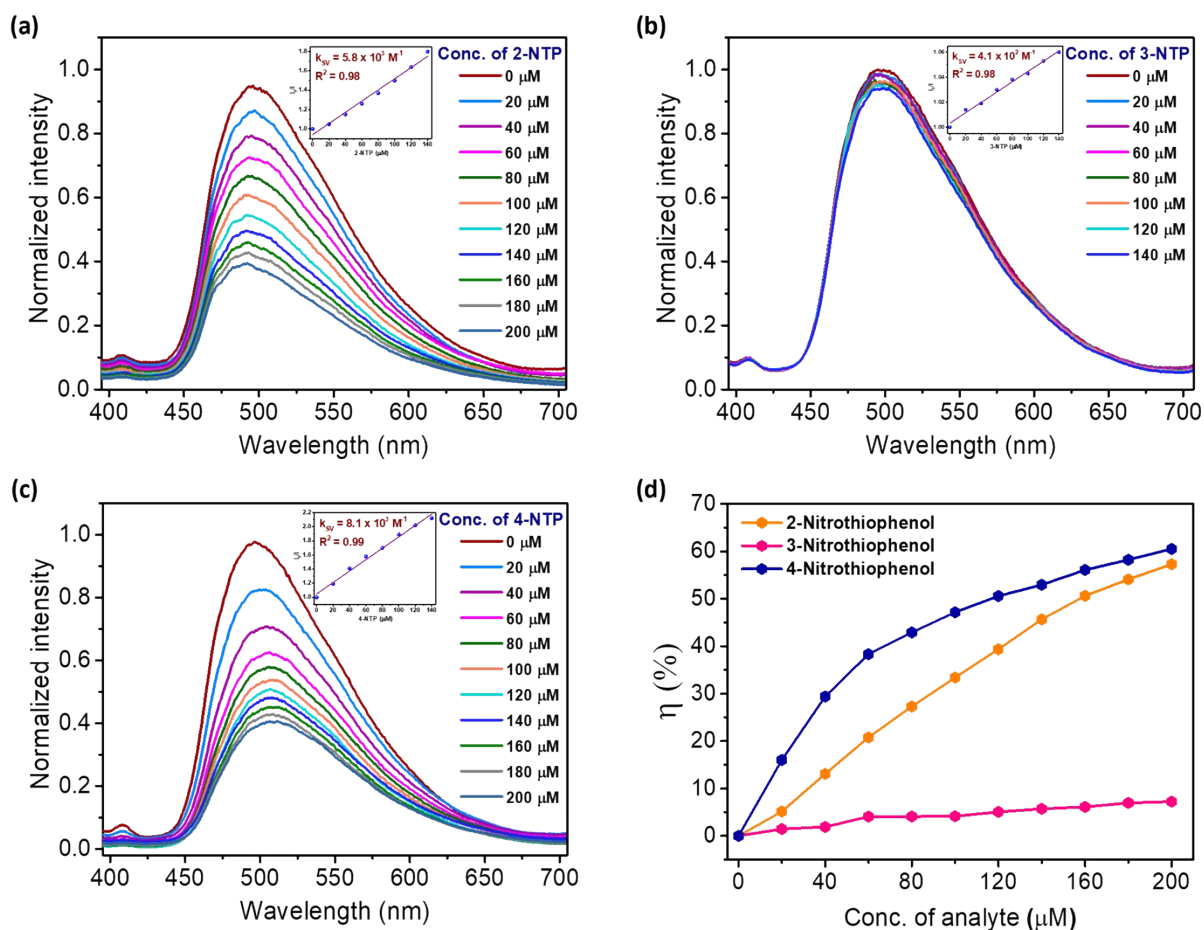


Fig. S15 Fluorescence quenching spectra of **TOITP** suspension with increasing concentrations of nitrothiophenols (NTPs) in methanol for excitation at 370 nm and their Stern-Volmer plots, (a) 2-nitrothiophenol (2-NTP), (b) 3-nitrothiophenol (3-NTP), and (c) 4-nitrothiophenol (4-NTP). (d) Quenching efficiencies of NTPs.

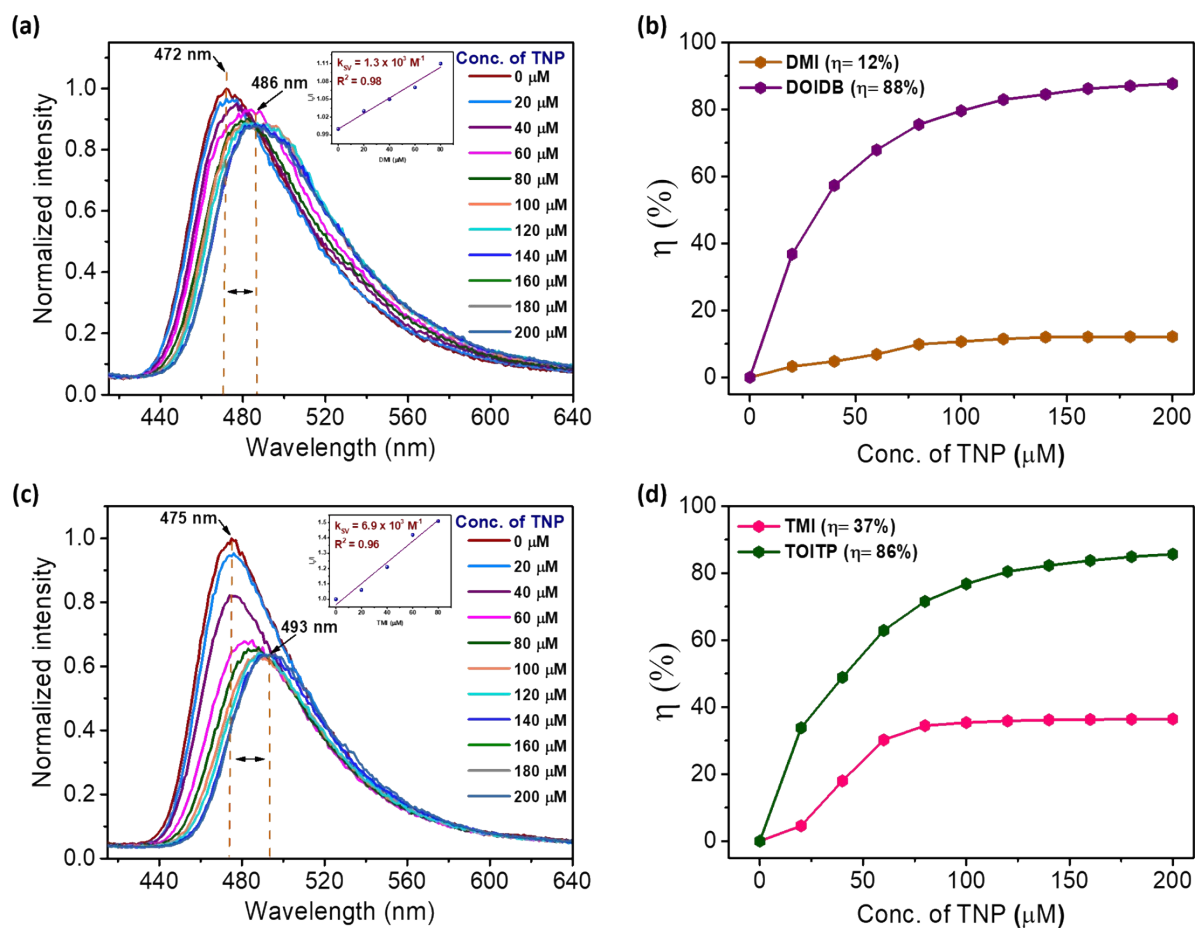


Fig. S16 (a) Fluorescence quenching spectra of **DMI** solution in methanol for excitation at 390 nm with TNP and corresponding Stern-Volmer plot. (b) Quenching efficiencies of **DMI** and **DOIDB**. (c) Fluorescence quenching spectra of the solution of **TMI** in methanol for excitation at 390 nm with TNP and corresponding Stern-Volmer plot. (d) Quenching efficiencies of **TMI** and **TOITP**.

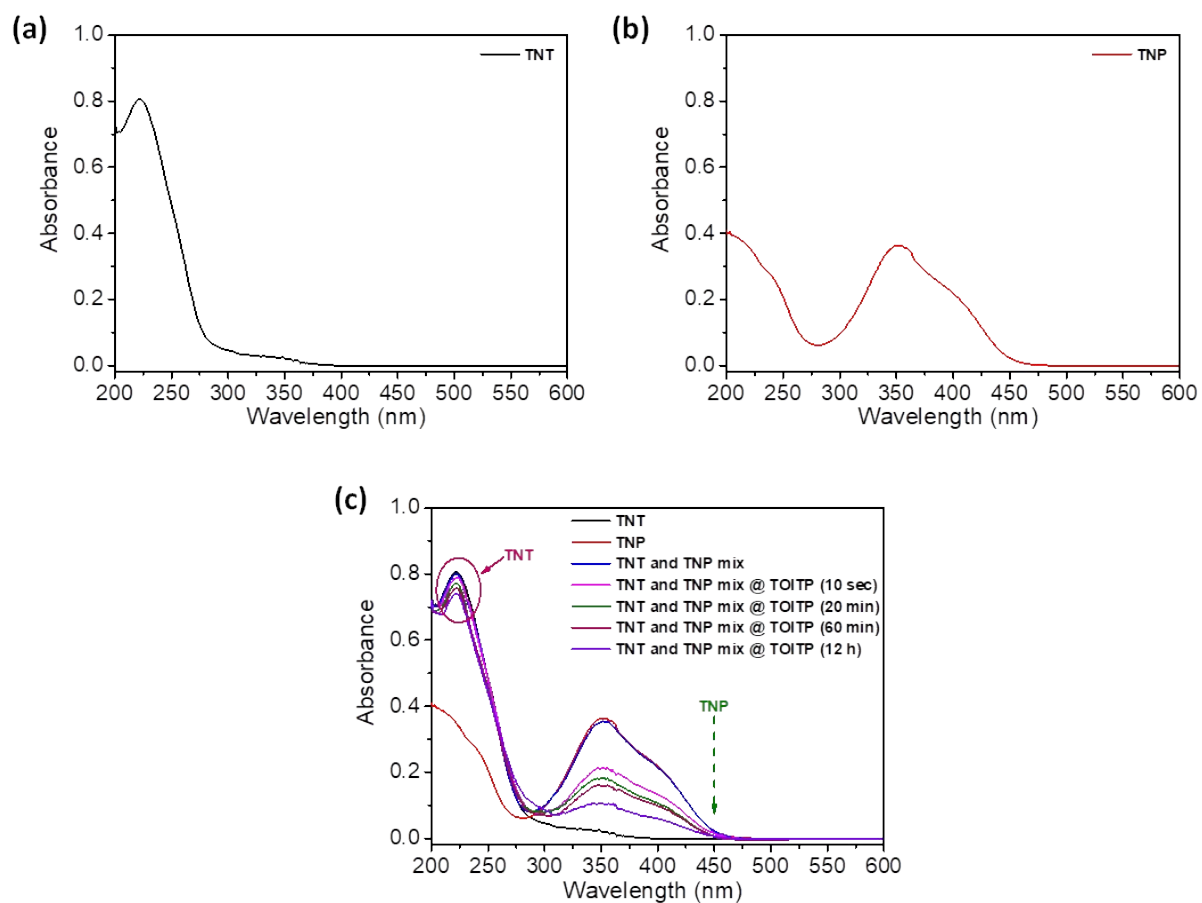
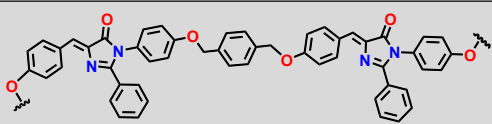
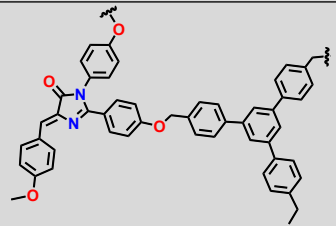
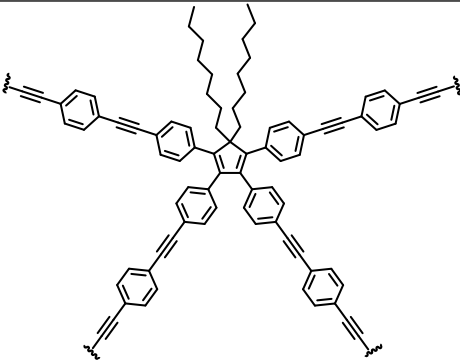
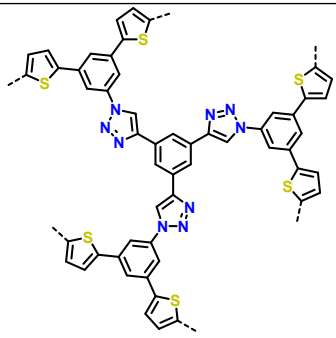
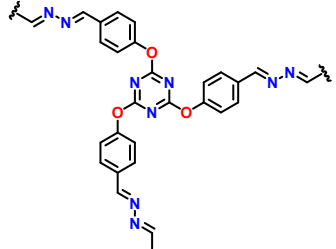


Fig. S17 (a) and (b) UV-vis absorption spectra of equimolar concentrations of TNT and TNP in MeOH, respectively. (c) Selective absorption of TNP over TNT by **TOITP** polymer in a solution containing equimolar concentrations of TNT and TNP in MeOH at different time intervals.

Table S1. Comparison of the performances of **DOIDB** and **TOITP** polymers in sensing of 4-nitroaniline with those of other materials reported previously in the literature.

S. No.	Material	LOD	Ksv (M ⁻¹)	Reference
COPs and POPs				
1.	 <p style="text-align: center;">DOIDB</p>	4.8×10 ⁻⁷ M (66 ppb)	4.9×10 ⁴	Present work
2.	 <p style="text-align: center;">TOITP</p>	4.5×10 ⁻⁷ M (62 ppb)	2.9×10 ⁴	Present work
3.	 <p style="text-align: center;">TPDC-DB</p>	455 ppb	1.7×10 ⁴	4
4.	 <p style="text-align: center;">PTPTB</p>	4.2×10 ⁻⁶ M	7.08 × 10 ⁴	5
5.	 <p style="text-align: center;">ANCOF</p>	89 ppb	8.37×10 ⁴	6

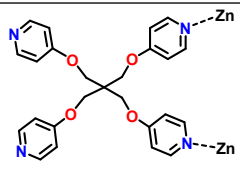
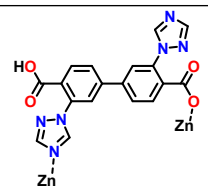
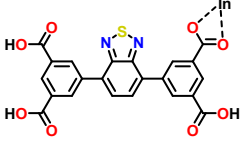
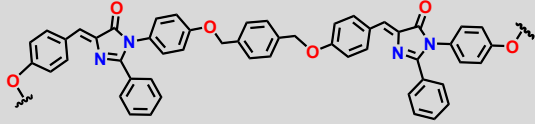
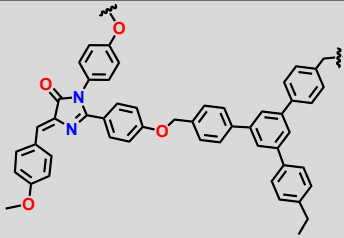
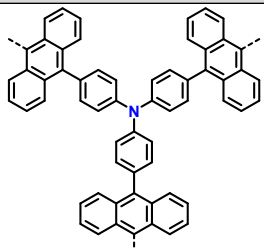
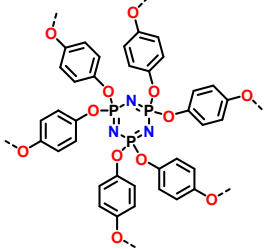
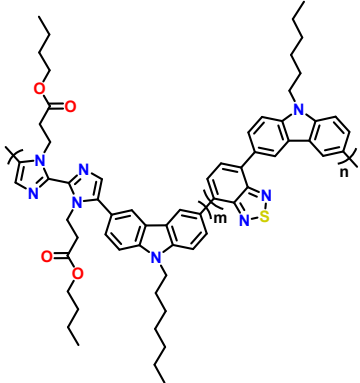
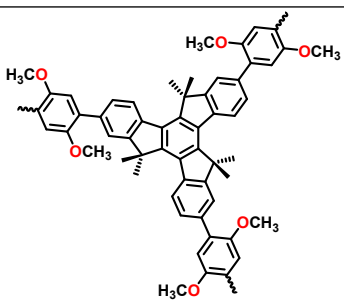
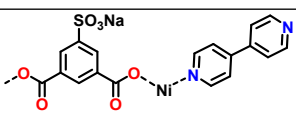
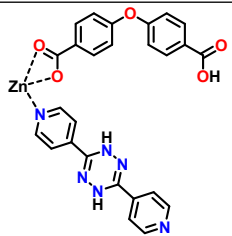
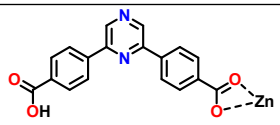
MOFs				
6.	 <p>$\{Zn_4(TPOM)(1,4-NDC)_4\}_n$</p>	88 ppb	7.87×10^4	7
7.	 <p>FJI-H26</p>	0.025 mM	4.1×10^4	8
8.	 <p>In-BTDI</p>	240 ppb	2.75×10^4	9

Table S2. Comparison of the performances of **DOIDB** and **TOITP** polymers in sensing of TNP with those of other materials reported previously in the literature.

S. No.	Material	LOD	Ksv (M ⁻¹)	Reference
COPs and POPs				
1.	 <p>DOIDB</p>	2.7×10 ⁻⁶ M (0.62 ppm)	4.1×10 ⁴	Present work
2.	 <p>TOITP</p>	2.28×10 ⁻⁶ M (0.52 ppm)	3.5×10 ⁴	Present work
3.	 <p>PTPA-AN-9,10</p>	3.4×10 ⁻⁵ M	5.8×10 ³	10
4.	 <p>HHQ</p>	1.30×10 ⁻¹¹ M	2.30×10 ⁵	11
5.	 <p>P1</p>	5.1×10 ⁻⁷ M	3.4×10 ⁴	12

6.	 <p>Tx-CMP-2</p>	$4.05 \times 10^{-9} \text{ M}$	7.35×10^4	13
MOFs				
7.	 <p>Ni-SIP-BPY</p>	87 ppb	6.7×10^6	14
8.	 <p>TMU-34</p>	$8.1 \times 10^{-6} \text{ M}$	1.8×10^6	15
9.	 <p>JLU-MOF109</p>	$1 \times 10^{-6} \text{ M}$	4.4×10^4	16

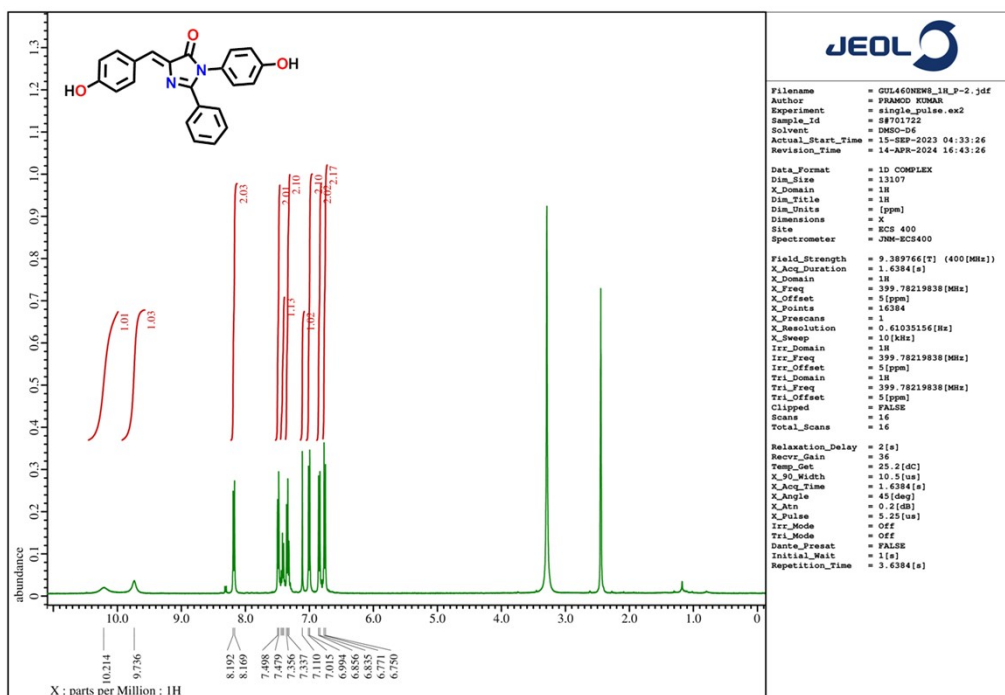


Fig. S18 ^1H NMR (400 MHz) spectrum of **3** in $\text{DMSO-}d_6$.

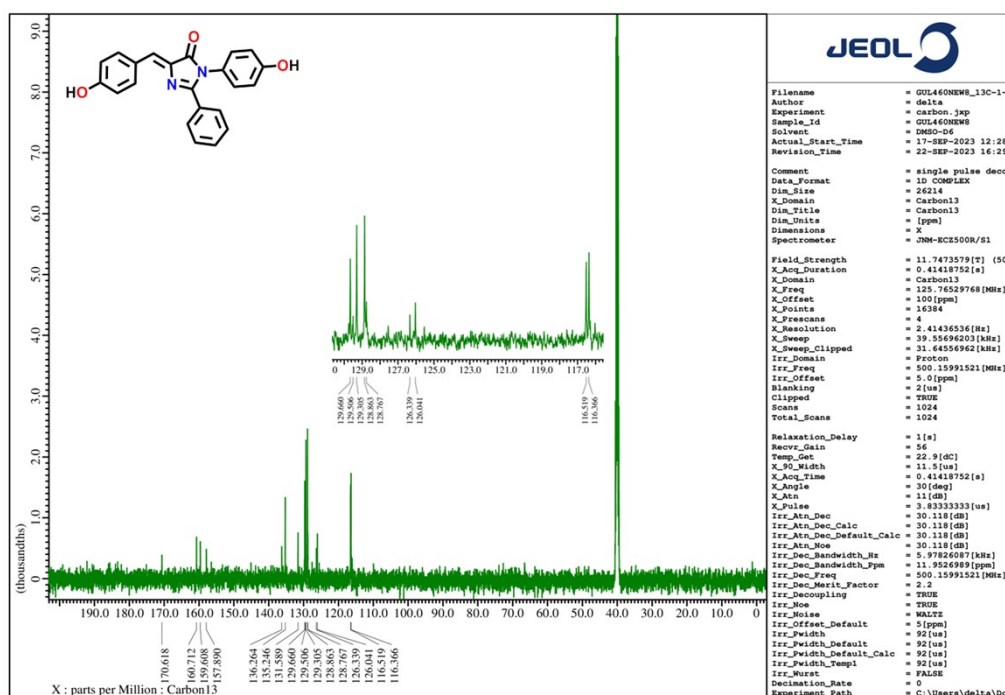


Fig. S19 $^{13}\text{C}\{^1\text{H}\}$ NMR (125 MHz) spectrum of **3** in $\text{DMSO-}d_6$.

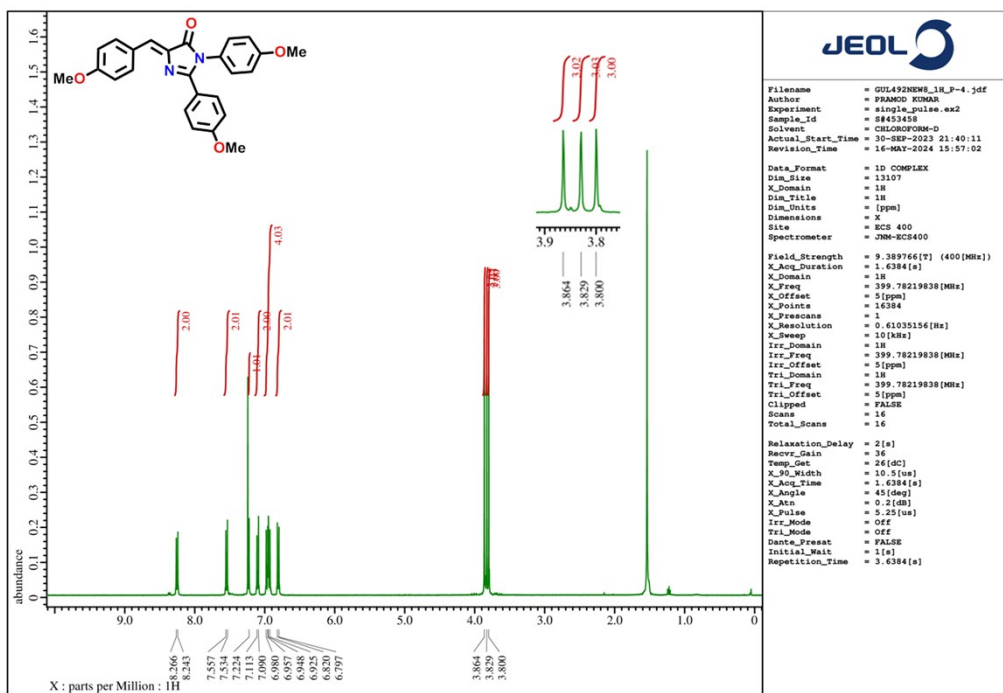


Fig. S20 ^1H NMR (400 MHz) spectrum of **6** in CDCl_3 .

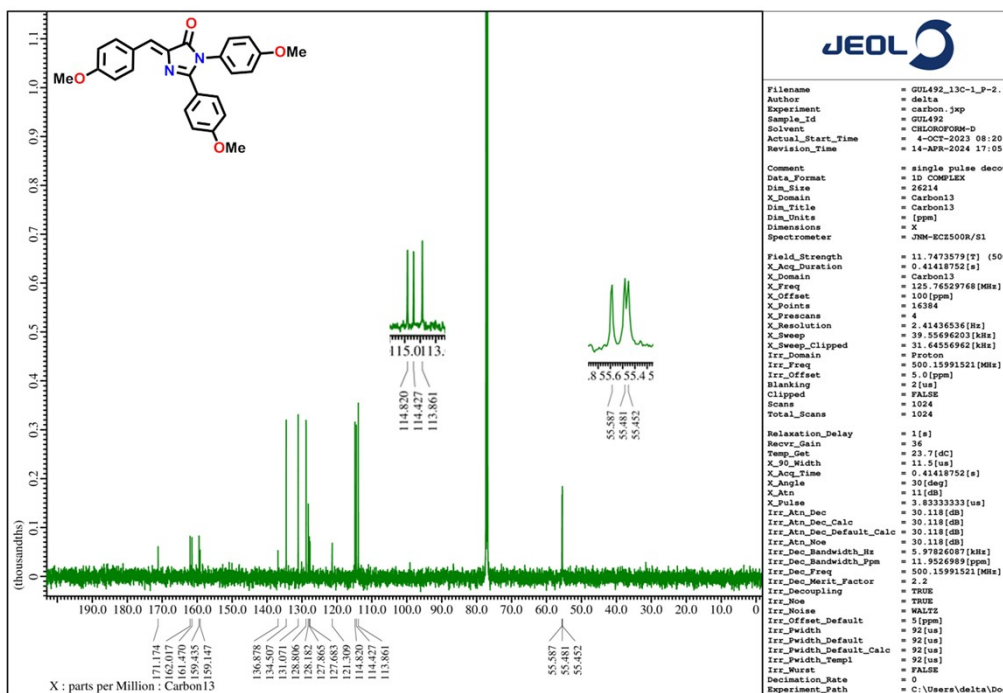


Fig. S21 $^{13}\text{C}\{^1\text{H}\}$ NMR (125 MHz) spectrum of **6** in CDCl_3 .

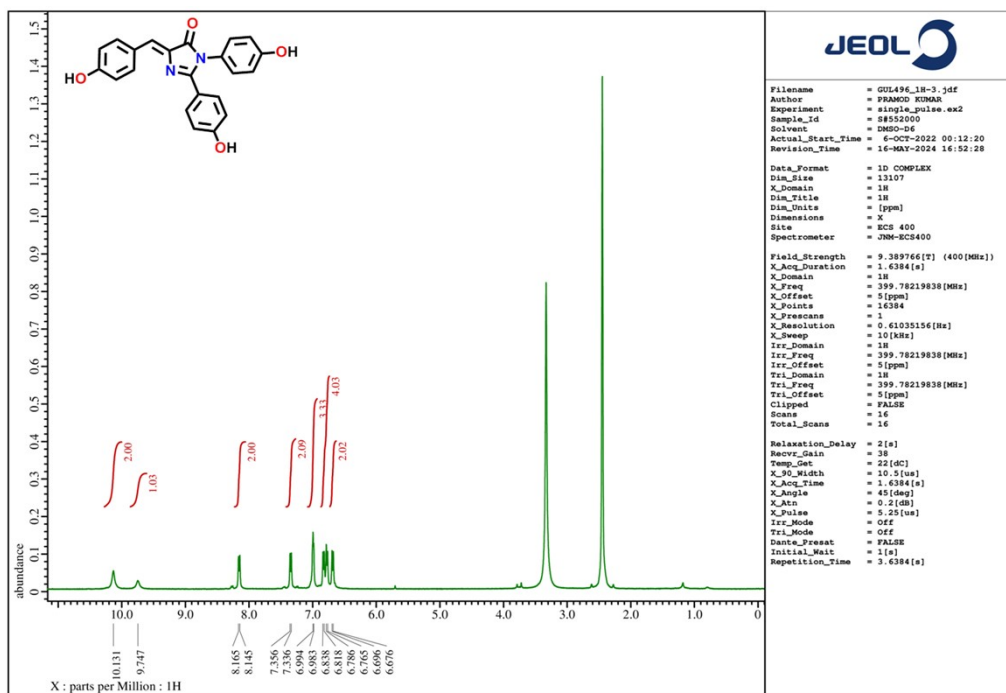


Fig. S22 ^1H NMR (400 MHz) spectrum of 7 in $\text{DMSO-}d_6$.

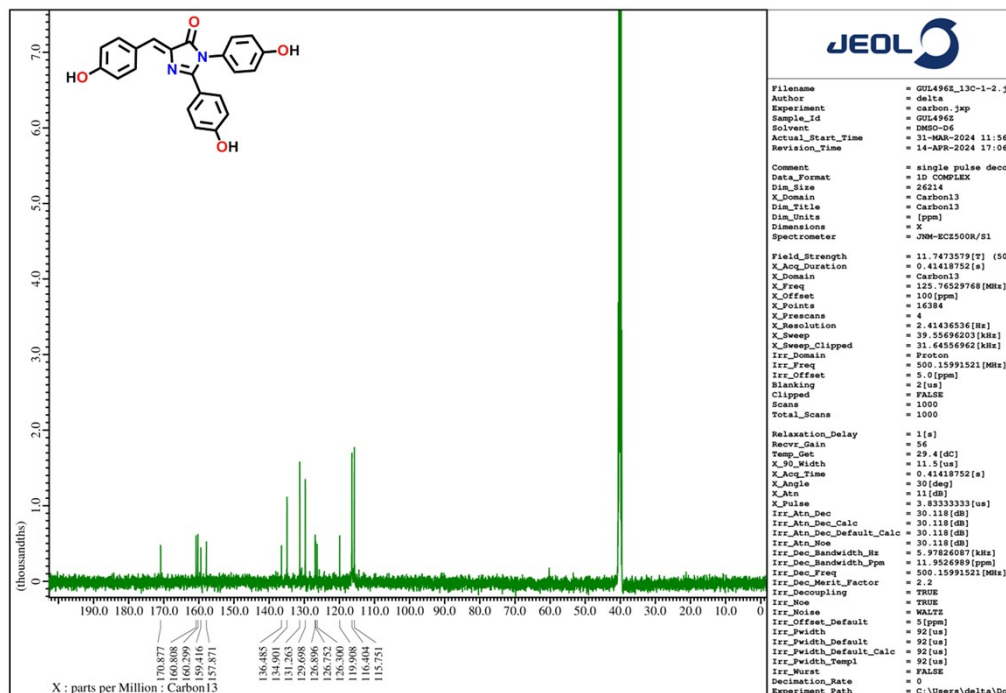


Fig. S23 $^{13}\text{C}\{^1\text{H}\}$ NMR (125 MHz) spectrum of 7 in $\text{DMSO-}d_6$.

References

1. C. I. C. Esteves, I. da Silva Fonseca, J. Rocha, A. M. S. Silva and S. Guieu, *Dyes Pigments*, 2020, **177**, 108267.
2. C. Voosala, P. S. Kilaru and U. K. Dasari, *J. Chin. Chem. Soc.*, 2016, **63**, 909–916.
3. G. Mariappan, B. P. Saha, S. Datta, D. Kumar and P. K. Haldar, *J. Chem. Sci.*, 2011, **123**, 335–341.
4. A. Deshmukh, S. Bandyopadhyay, A. James and A. Patra, *J. Mater. Chem. C*, 2016, **4**, 4427–4433.
5. F. Wei, X. Cai, J. Nie, F. Wang, C. Lu, G. Yang, Z. Chen, C. Ma and Y. Zhang, *Polym. Chem.*, 2018, **27**, 3832–3839.
6. P. Das, G. Chakraborty and S. K. Mandal, *ACS Appl. Mater. Interfaces*, 2020, **12**, 10224–10232.
7. G. Chakraborty, P. Das and S. K. Mandal, *ACS Appl. Mater. Interfaces*, 2018, **10**, 42406–42416.
8. D. Wu, K. Zhou, J. Tian, C. Liu, F. Jiang, D. Yuan, Q. Chen and M. Hong, *Journal of Materials Chemistry C*, 2020, **8**(29), 9828–9835.
9. Z. Zhang, Z. Wu, Z. Li, Y. Zhao, M. Yu, F. Jiang, L. Chen and M. Hong, *Crystal Growth & Design*, 2023, **23** (6), 4491–4498.
10. S. Sau, F. Banerjee and S. K. Samanta, *ACS Appl. Nano Mater.*, 2023, **6**, 11679–11688.
11. T-M. Geng, M. Liu and C. Hu, H. Zhu, *New Journal of Chemistry*, 2021, **45**, 3007–3013.
12. T. Wang, N. Zhang, R. Bai and Y. Bao, *J. Mater. Chem. C*, 2018, **6**, 266–270.
13. Y. Nailwal, M. Devi and S. K Pal, *ACS Appl. Polym. Mater.*, 2022, **4**, 2648–2655.
14. S. Bhattacharjee, S. Bera, R. Das, D. Chakraborty, A. Basu, P. Banerjee, S. Ghosh and A. Bhaumik, *ACS Appl. Mater. Interfaces*, 2022, **14**, 20907–20918.
15. S. A. A. Razavi, A. Morsali, M. Piroozzadeh, *Inorg. Chem.*, 2022, **61**, 7820–7834.
16. W. Liu, J. Qiao, J. Gu, Y. Liu, *Inorg. Chem.* 2023, **62**, 1272–1278.